

# Blind Detection-Estimation and Performance Characterization in Cell-Free Massive MIMO

Aditya Sarkar, Sk Md Shafique Anwar, Adarsh Patel

School of Computing and Electrical Engineering (SCEE), Indian Institute of Technology Mandi, H.P. India

Email: b19003@students.iitmandi.ac.in, s23113@students.iitmandi.ac.in, adarsh@iitmandi.ac.in

**Abstract**—This work investigates the uplink of a cell-free massive multiple-input multiple-output (MIMO) system, with particular emphasis on the encoded transmission of data from user equipment (UE) to distributed access points (APs). The APs forward their processed signals to a central processing unit (CPU), where joint channel estimation and data detection are performed without any a priori knowledge of the channel coefficients, channel statistics, or user data. A generalized mathematical framework for a cell-free massive MIMO system is developed. Within this framework, the multiway unified detection and estimation (MUDE) algorithm is proposed for simultaneous estimation of the uplink channels and recovery of the user data. The MUDE scheme requires only a single reference/pilot bit per UE. Further, analytical expressions for the Cramer-Rao Lower Bound (CRLB) and achievable rate bounds are derived for the defined setting. Finally, numerical simulation results are presented to evaluate the performance of the proposed MUDE scheme in comparison with conventional baseline approaches, including zero-forcing (ZF) and ZF combined with pilot-assisted channel estimation.

**Index Terms**—CPD, Least squares, cell-free massive MIMO

## I. INTRODUCTION

Modern wireless systems are moving away from the idea of cells and toward architectures that provide seamless service over large areas. The cell-free massive MIMO (CF-mMIMO) [1] framework is a well-known example. In this framework, many access points (APs) are spread out across the coverage area. Instead of putting users in fixed cells, these APs work together to help each user equipment (UE), either as a group or through a subset chosen by the network, depending on how the system is set up. In operation, UEs send data that is first picked up by nearby APs and then sent to a central processing unit (CPU) over the fronthaul links. When the system uses centralized processing, this CPU has to do heavy tasks like estimating channels and detecting data symbols [2]. Distributed processing is another option. Some of the signal processing is done directly at the APs, which makes the CPU's job easier and allows for more scalable deployments. Recent research has investigated radio-stripe implementations [3] that integrate access points within adaptable wiring frameworks, promising easier installation, better coordination, and a more practical way to make large-scale distributed MIMO systems work.

In the centralized scheme, when the APs are spread out, they do not all contribute equally to the channel. APs that are farther away from a user only provide small gains, which weakens the channel-hardening effect that usually makes processing easier

in cell free massive MIMO. This makes channel estimation a task that requires the system to learn a lot of coefficients. In this two-hop architecture, information goes from UEs to APs and then from APs to the CPU, which necessitates that the whole network is perfectly synchronized. The choice of methodology for detection or estimation comes after dealing with these built-in limits. Traditional schemes use uplink pilots to explicitly estimate the channel before decoding [4], which makes the pilot overhead higher [1], [5] and can also introduce pilot contamination issues [6]. Blind detection, on the other hand, does not use dedicated pilots. Instead, it infers both the data and the channel at the same time, which is a more efficient use of resources, reported in existing literature such as [7], [8].

In the downlink scenario, [9] suggested a blind estimation method for a CF-mMIMO network by utilizing maximal ratio combining (MRC) and minimum mean squared error (MMSE) techniques, presuming that the channel and noise statistics are already known at the UE and that the coherence time is sufficiently long. [10] examined semi-blind techniques for joint data detection and channel estimation by utilizing the message passing (MP) algorithm, which alternates between these two sub-problems of estimation and detection, and exploiting channel's sparseness. Channel data are presumed to be known at the receiver in both of these work. Expectation Propagation (EP)-based techniques for semi-blind detection in CF-mMIMO networks have been introduced recently [11], [12]. These methods use Bayesian priors and iterative MP to jointly improve channel and data estimates with reduced pilot overhead. To the best of our knowledge, no work examines the system in which the receiver is unaware of the channel statistics or coefficients.

Unlike the methods discussed tensor signal processing can capture multi-dimensional dependencies. In [13], [14], blind techniques combines limited prior information such as codebooks or pilot symbols with statistical inference from the received data using tensor decompositions. In [15], a Canonical Polyadic Decomposition (CPD)-based method was adopted in RIS-aided MIMO systems to improve estimation performance. In [16], Block Term Decomposition was applied within the joint framework for uniform linear array configurations. This study exploits tensor signal processing especially CPD to represents the uplink cell-free massive MIMO system model. The key contribution of this study are,

- the uplink cell-free massive MIMO system model is presented and the lower bounds on the probability of

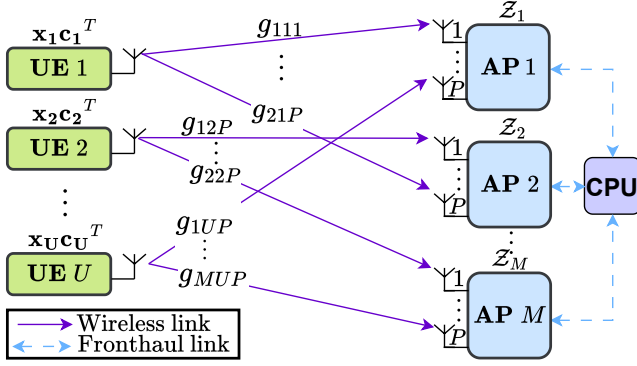


Fig. 1: Uplink CF-mMIMO system model with  $U$  users and  $M$  APs with  $P$  antennas each, connected to the CPU via fronthaul.

error in detection and the mean squared error for channel estimation are derived.

- A novel joint estimation and detection algorithm, Multi-way Unified Detection and Estimation (MUDE) utilizing single pilot bit per user, is proposed for the cell-free massive MIMO systems and compared with the state of the art detectors.

The rest of the paper is structured as follows: Section II describes the uplink CF-mMIMO system model, Section III derives the probability of error (PoE) and minimum mean squared error (MMSE) bound expression for data and channel estimates respectively. Section IV presents the proposed MUDE method along with its algorithm. Section V contains simulation comparisons, and Section VI provides conclusions. *Notations*: lower case and upper case bold letters are used to show column vectors and matrices, respectively. Calligraphic letters are used to show tensors. The symbols  $\diamond$ , and  $\circ$  stand for the Khatri–Rao product and the outer product, respectively. The Moore–Penrose pseudoinverse is shown by the symbol  $(\cdot)^\dagger$ , and the transpose and conjugate transpose are shown by the superscripts  $(\cdot)^T$  and  $(\cdot)^H$ . The expectation operator is written as  $\mathbb{E}\{\cdot\}$ , the trace operator as  $\text{tr}(\cdot)$ , and the Frobenius norm as  $\|\cdot\|_F$ . A complex Gaussian random variable in the multivariate context,  $\mathbf{x} \sim \mathcal{CN}(\boldsymbol{\mu}, \boldsymbol{\Sigma})$  signifies a complex Gaussian vector characterized by mean vector  $\boldsymbol{\mu}$  and covariance matrix  $\boldsymbol{\Sigma}$ .

## II. SYSTEM MODEL

Consider a time-division duplex (TDD) coherent multiple access channel (MAC), i.e., using same time–frequency resources, CF-mMIMO network, as depicted in Fig. 1, comprising  $M$  access points (APs), each equipped with  $P$  antennas and jointly serving  $U$  single-antenna user equipments (UEs), under the regime  $MP \gg U$ . The APs are connected to a central processing unit (CPU) via fronthaul links that are assumed to provide sufficiently large capacity to enable error-free data transmission.

The data associated with UE  $u$ , for  $1 \leq u \leq U$ , is modeled by the vector  $\mathbf{x}_u \in \mathbb{R}^{T \times 1}$ , where each coherence block comprises  $T$  symbol intervals. The corresponding encoded

data symbol matrix  $\mathbf{B}_u \in \mathbb{R}^{T \times Q}$  for UE  $u$  is obtained as the outer product between the data vector  $\mathbf{x}_u$  and the encoding vector  $\mathbf{c}_u \in \mathbb{R}^{Q \times 1}$ , with  $Q \geq U$ , and is defined as

$$\begin{aligned} \mathbf{B}_u &= \mathbf{x}_u \mathbf{c}_u^T \\ &= \mathbf{x}_u \circ \mathbf{c}_u, \end{aligned} \quad (1)$$

Let  $\mathbf{g}_{mu} \in \mathbb{C}^{P \times 1}$  denote the channel coefficient vector between the  $P$  antennas of AP  $m$ ,  $1 \leq m \leq M$ , and UE  $u$  where  $g_{mup} \in \mathbb{C}$  denotes the element  $p$  of the vector  $\mathbf{g}_{mu}$ . The vector  $\mathbf{g}_{mu}$  is modeled as a complex Gaussian random vector,  $\mathbf{g}_{mu} \sim \mathcal{CN}(\mathbf{0}_P, \mathbf{R}_{mu})$ , with zero-mean vector  $\mathbf{0}_P \in \mathbb{R}^{P \times 1}$  whose entries are all equal to zero. The statistical spatial correlation matrix  $\mathbf{R}_{mu} \in \mathbb{C}^{P \times P}$  characterizes large-scale fading, spatial channel correlation, path loss, and shadowing effects. The received signal  $\mathbf{z}_{mp} \in \mathbb{C}^{T \times Q}$  at antenna  $p$  of AP  $m$  from  $U$  users corresponding to the transmission of the encoded data symbol matrix  $\mathbf{B}_u \in \mathbb{R}^{T \times Q}$  in (1) is defined as

$$\begin{aligned} \mathbf{z}_{mp} &= \sum_{u=1}^U g_{mup} \mathbf{B}_u + \mathbf{W}_{mp} \\ &= \sum_{u=1}^U g_{mup} (\mathbf{x}_u \circ \mathbf{c}_u) + \mathbf{W}_{mp}, \end{aligned}$$

where  $\mathbf{W}_{mp} \in \mathbb{C}^{T \times Q}$  is an additive white Gaussian (AWG) noise matrix with independent and identically distributed (i.i.d.) entries  $\mathcal{CN}(0, \sigma^2)$ . The received signal tensor  $\mathcal{Z}_m \in \mathbb{C}^{P \times T \times Q}$  at AP  $m$  is obtained by stacking  $\mathbf{z}_{mp}$  along  $P$  antennas, i.e., stack the matrices  $\{\mathbf{z}_{m1} \dots \mathbf{z}_{mp} \dots \mathbf{z}_{mP}\}$  along  $p$ , given as

$$\mathcal{Z}_m = \sum_{u=1}^U \mathbf{g}_{mu} \circ \mathbf{x}_u \circ \mathbf{c}_u + \mathcal{W}_m. \quad (2)$$

Similarly, the noise matrices  $\{\mathbf{W}_{m1} \dots \mathbf{W}_{mp} \dots \mathbf{W}_{mP}\}$  are stacked along the index  $p$  to form the noise tensor  $\mathcal{W}_m \in \mathbb{C}^{P \times T \times Q}$ . Subsequently, the received tensors  $\mathcal{Z}_m$ ,  $1 \leq m \leq M$ , are concatenated to construct the composite baseband system model associated with the  $MP$  receive antennas,  $T$  symbol intervals, and  $U$  UEs in the CF-mMIMO communication network, given by

$$\begin{aligned} \mathcal{Z} &= \sum_{u=1}^U \mathbf{g}_u \circ \mathbf{x}_u \circ \mathbf{c}_u + \mathcal{W} \\ &= \mathbf{G} \circ \mathbf{X} \circ \mathbf{C} + \mathcal{W}, \end{aligned} \quad (3)$$

where the noise  $\mathcal{W}$ , is formed similarly by concatenating the tensors  $\mathcal{W}_m$ . Let  $\mathbf{G} = [\mathbf{G}_1, \mathbf{G}_2, \dots, \mathbf{G}_M] \in \mathbb{C}^{MP \times U}$  where  $\mathbf{G}_m = [\mathbf{g}_{m1}, \mathbf{g}_{m2}, \dots, \mathbf{g}_{mU}] \in \mathbb{C}^{P \times U}$ ,  $\mathbf{X} = [\mathbf{x}_1, \mathbf{x}_2, \dots, \mathbf{x}_U] \in \mathbb{R}^{T \times U}$ , and  $\mathbf{C} = [\mathbf{c}_1, \mathbf{c}_2, \dots, \mathbf{c}_U] \in \mathbb{R}^{Q \times U}$ . The subsequent section derives upper bounds on the performance of detection and estimation procedures in CF-mMIMO systems.

### III. PERFORMANCE CHARACTERIZATION

#### A. Probability of Error in Data Detection

The data detection performance is assessed in terms of the probability of error (PoE), defined as the ratio of incorrectly decoded data bits to the total number of transmitted data bits. Let  $\Theta = (\mathbf{G} \diamond \mathbf{C}) \in \mathbb{C}^{MPQ \times U}$ . The estimate of  $\mathbf{X}$  is then obtained by first performing a mode-2 matricization [17], [18] of (3) as

$$\begin{aligned} \mathbf{Z}_{(2)} &= \mathbf{X}(\mathbf{G} \diamond \mathbf{C})^H + \mathbf{W}_{(2)} \\ &= \mathbf{X}(\Theta)^H + \mathbf{W}_{(2)}, \end{aligned} \quad (4)$$

where (4) follows from the substitution  $\Theta = \mathbf{G} \diamond \mathbf{C}$ . Solving for the decoded signal  $\hat{\mathbf{X}}$  in (4), applying Zero-Forcing (ZF), results in

$$\hat{\mathbf{X}} = \hat{\mathbf{X}}_{ZF} = [\mathbf{Z}_{(2)}(\Theta^H)^\dagger]_{+1/-1}, \quad (5)$$

where the operator  $[a]_{+1/-1}$  in (5) outputs  $+1$  if  $\Re(\mathbf{a}) \geq 0$  and  $-1$  if  $\Re(\mathbf{a}) < 0$ . Thus,  $\hat{\mathbf{X}} \in \{+1, -1\}^{T \times U}$ . Data detection is performed with minimum probability of error (PoE) when the channel is perfectly estimated at the receiver. The following theorem, together with its subsequent proof, presents the corresponding derivation in the context of a cell-free massive MIMO system.

**Theorem III.1.** *The Minimum expected probability of error (PoE) in data  $\mathbf{X}$  detection (5) for such a coherent MAC based CF-mMIMO system in (3) in the uplink, when the channel  $\mathbf{G}$  is perfectly known at the receiver, is given as*

$$\begin{aligned} \mathbb{E}[P_e] &= \left[ \frac{1}{2} \left( 1 - \sqrt{\frac{\rho}{1+\rho}} \right) \right]^{MPQ-U+1} \\ &\times \sum_{n=0}^{MPQ-U+1} \binom{MPQ-U+n}{n} \left( \frac{1 + \sqrt{\frac{\rho}{1+\rho}}}{2} \right)^n, \end{aligned} \quad (6)$$

where  $\rho$  is signal-to-noise ratio (SNR) and is given as follows

$$\rho = \frac{1}{\sigma^2}. \quad (7)$$

*Proof.* On post-multiply (4) by  $(\Theta^H)^\dagger$ , yields

$$\begin{aligned} \mathbf{Z}_{(2)}(\Theta^H)^\dagger &= \mathbf{X}(\Theta)^H(\Theta^H)^\dagger + \mathbf{W}_{(2)}(\Theta^H)^\dagger \\ \tilde{\mathbf{Z}}_{(2)} &= \mathbf{X} + \tilde{\mathbf{W}}_{(2)}, \end{aligned} \quad (8)$$

where  $\tilde{\mathbf{Z}}_{(2)} = \mathbf{Z}_{(2)}(\Theta^H)^\dagger \in \mathbb{C}^{T \times U}$  and  $\tilde{\mathbf{W}}_{(2)} = \mathbf{W}_{(2)}(\Theta^H)^\dagger \in \mathbb{C}^{T \times U}$ .  $\Theta = \mathbf{G} \diamond \mathbf{C}$  is khatri-rao product of the perfectly known channel and code matrix. The subscript (2) is dropped because it remains the same in the subsequent text. For UE  $u$  and bit  $t$ , is given as

$$\tilde{\mathbf{Z}}_{tu} = \mathbf{X}_{tu} + \tilde{\mathbf{W}}_{tu}. \quad (9)$$

Now  $p(\tilde{\mathbf{Z}}_{tu} | \mathbf{X}_{tu} = +1) \sim \mathcal{CN}(1, \mathbb{E}\{\tilde{\mathbf{W}}_{tu} \tilde{\mathbf{W}}_{tu}^*\})$  and  $p(\tilde{\mathbf{Z}}_{tu} | \mathbf{X}_{tu} = -1) \sim \mathcal{CN}(-1, \mathbb{E}\{\tilde{\mathbf{W}}_{tu} \tilde{\mathbf{W}}_{tu}^*\})$ . The following two hypotheses given as

- 1)  $\mathcal{H}_0$ :  $\mathbf{X}_{tu} = +1$ ,
- 2)  $\mathcal{H}_1$ :  $\mathbf{X}_{tu} = -1$ .

Since Zero-Forcing is used to detect  $\mathbf{X}$ , if  $\|\tilde{\mathbf{Z}}_{tu} - 1\|_F^2 < \|\tilde{\mathbf{Z}}_{tu} + 1\|_F^2$ , then  $\mathcal{H}_0$  is accepted, otherwise  $\mathcal{H}_1$ . The resultant test statistic is  $\tilde{\mathbf{Z}}_{tu} > 0$  on simplifying it. Now the probability of error is given by,

$$\begin{aligned} P_e &= 0.5(p(\hat{\mathbf{X}}_{tu} = +1 | \mathbf{X}_{tu} = -1) + p(\hat{\mathbf{X}}_{tu} = -1 | \mathbf{X}_{tu} = +1)) \\ &= 0.5(p(\tilde{\mathbf{Z}}_{tu} > 0 | \mathbf{X}_{tu} = -1) + p(\tilde{\mathbf{Z}}_{tu} < 0 | \mathbf{X}_{tu} = +1)). \end{aligned}$$

Since noise random variables are i.i.d., the distribution of  $\tilde{\mathbf{W}}_{tu}$  can be computed as follows,

$$\begin{aligned} \tilde{\mathbf{W}}_{tu} &= \sum_{i=1}^{MPQ} \mathbf{W}_{ti}((\Theta^H)^\dagger)_{iu}, \\ \tilde{\mathbf{W}}_{tu} &\sim \mathcal{CN}\left(0, \sum_{i=1}^{MPQ} ((\Theta^\dagger)_{ui}(\Theta^\dagger)_{iu}^* \sigma^2)\right). \end{aligned} \quad (10)$$

It is easy to note that  $\sum_{i=1}^{MPQ} ((\Theta^\dagger)_{ui}(\Theta^\dagger)_{iu}^* \sigma^2) = (\Theta^H \Theta)_{uu}^\dagger \sigma^2$ . So  $\tilde{\mathbf{W}}_{tu} \sim \mathcal{CN}(0, (\Theta^H \Theta)_{uu}^\dagger \sigma^2)$ . Therefore, PoE can be written as

$$P_e = Q\left(\frac{1}{(\Theta^H \Theta)_{uu}^{-1/2} \sigma}\right) = Q\left(\frac{\sqrt{\rho}}{(\Theta^H \Theta)_{uu}^{-1/2}}\right),$$

where  $Q(\cdot)$  is the Q-function which is given as -

$$Q(x) = \frac{1}{\sqrt{2\pi}} \int_x^\infty e^{-t^2/2} dt, \quad (11)$$

Here  $(\Theta^H \Theta)_{uu}^{-1} \in \mathbb{C}$  is the  $u$ th diagonal element of  $(\Theta^H \Theta)^{-1}$  and is a random variable because  $\mathbf{G}$  varies over time. Since column  $u$  of  $\mathbf{G}$ ,  $\mathbf{G}_u \sim \mathcal{CN}(\mathbf{0}, \mathbf{R}_u)$  where  $\mathbf{R}_u \in \mathbb{C}^{MP \times MP}$  is the correlation matrix,  $u$ th column of  $\Theta$ ,  $\Theta_u \sim \mathcal{CN}(\mathbf{0}, \mathbf{R})$ , where  $\mathbf{R} \in \mathbb{C}^{UMP \times UMP}$  is block diagonal of  $[\mathbf{R}_u, \mathbf{R}_u, \dots, \mathbf{R}_u]$  because  $\Theta_u = \mathbf{C}_u \diamond \mathbf{G}_u$ . Expected PoE can be calculated as

$$\mathbb{E}[P_e] = \int_{-\infty}^\infty Q(\sqrt{\rho \lambda_u}) F_{\lambda_u}(\lambda_u) d\lambda_u, \quad (12)$$

where  $\lambda_u = (\Theta^H \Theta)_{uu}^{-1}$ . It can be further simplified using Schur's complement and is written below as

$$\begin{aligned} \lambda_u &= (\Theta_u^H \Theta_u - \Theta_u^H (\Theta_{-u} (\Theta_{-u}^H \Theta_{-u})^{-1} \Theta_{-u}^H) \Theta_u) \\ &= \Theta_u^H (\mathbf{I} - \mathcal{Q}) \Theta_u \end{aligned} \quad (13)$$

where  $\mathcal{Q} = \Theta_{-u} (\Theta_{-u}^H \Theta_{-u})^{-1} \Theta_{-u}^H$ . Note that  $\mathcal{Q}$  is idempotent, so  $\mathbf{I} - \mathcal{Q}$  is also idempotent. Using result in [19],  $F_{\lambda_u}(\lambda_u) \sim \mathcal{X}^2(r)$  where  $r$  is the rank of  $\mathbf{I} - \mathcal{Q}$ . Assuming  $U < MPQ$ ,  $\mathcal{Q}$  projects on the column space of  $\Theta_{-u} \in \mathbb{C}^{MPQ \times (U-1)}$ . So,  $\mathbf{I} - \mathcal{Q}$  will project on the null space of  $\Theta_{-u}^H$ . Hence rank of  $\mathbf{I} - \mathcal{Q}$  is  $MPQ - (U - 1)$ . Since  $\mathbf{G}$  has both real and imaginary components, degree of freedom (DOF) of  $\chi^2$  distribution will be  $2(MPQ - U + 1)$ . Substituting these

values in (12) and integrating it over, expected minimum PoE can be obtained as

$$\begin{aligned} \mathbb{E}[P_e] &= \left[ \frac{1}{2} \left( 1 - \sqrt{\frac{\rho}{1+\rho}} \right) \right]^{MPQ-U+1} \\ &\times \sum_{n=0}^{MPQ-U+1} \binom{MPQ-U+n}{n} \left( \frac{1 + \sqrt{\frac{\rho}{1+\rho}}}{2} \right)^n. \end{aligned} \quad (14)$$

This completes the proof for theorem 1.  $\square$

### B. Mean Squared Error in Channel Estimation

In this section, the minimum mean squared error is determined that can be attained in the estimation of channel coefficients by computing the Cramer-Rao Lower Bound (CRLB).  $\mathbf{G}$  is estimated using Minimum Mean Squared Estimation (MMSE) as follows

$$\hat{\mathbf{G}} = \mathbb{E}[\mathbf{G}|\mathbf{Z}_{(1)}] \quad (15)$$

$$= \mathbf{Z}_{(1)}(\mathbf{X} \diamond \mathbf{C})^{T\dagger}. \quad (16)$$

Note that it is unbiased because  $\mathbb{E}[\hat{\mathbf{G}}] = \mathbf{G}$ . The following theorem and its proof outline the derivation of CRLB.

**Theorem III.2.** *The minimum mean-squared error in estimating the channel  $\mathbf{G}$  using (16) for the coherent CF-mMIMO uplink system in (3), when perfect knowledge of the  $U$  users' encoded data in (1) is available at the CPU, is given as*

$$\min_{\mathbf{G}} \mathbb{E}[\|\hat{\mathbf{G}} - \mathbf{G}\|_F^2] = 2MP\sigma^2 \text{tr}((\mathbf{X} \diamond \mathbf{C})^T (\mathbf{X} \diamond \mathbf{C}))^{-1}. \quad (17)$$

*Proof.* It can be proved by calculating the CRLB for (17). To do so, the log-likelihood is first computed as follows -

$$\log p(\mathbf{Z}_{(1)}; \mathbf{G}) = -\frac{1}{\sigma^2} \|\mathbf{Z}_{(1)} - \mathbf{G}(\mathbf{X} \diamond \mathbf{C})^T\|_F^2 + C, \quad (18)$$

where  $C$  consists of the constant terms and is not dependent on  $\mathbf{G}$ . Fisher Information Matrix (FIM) [20]  $\mathbf{J}_{\mathbf{G}}$  can now be computed as the block diagonal matrix with principle diagonal matrices  $\mathbf{A}$  and  $\mathbf{A}^*$ , i.e.,  $\mathbf{J}_{\mathbf{G}} = \text{diag}[\mathbf{A} \ \mathbf{A}^*] \in \mathbb{C}^{2MPU \times 2MPU}$ , where  $\mathbf{A} = (1/\sigma^2)(\mathbf{X} \diamond \mathbf{C})^T (\mathbf{X} \diamond \mathbf{C}) \otimes \mathbf{I}_{MP}$ . Then the  $\text{tr}(\mathbf{J}_{\mathbf{G}}^{-1})$  is computed as  $2MP\sigma^2 \times \text{tr}((\mathbf{X} \diamond \mathbf{C})^T (\mathbf{X} \diamond \mathbf{C}))^{-1}$ , gives the MMSE for the estimation of the unknown  $\mathbf{G}$  -this completes the proof.  $\mathbf{C}$  is assumed to be perfectly known at the receiver. If  $\mathbf{X}$  is decoded without error,  $\text{tr}(\mathbf{J}_{\mathbf{G}}^{-1})$  will be minimum.  $\square$

In the following section the proposed MUDE algorithm based on ALS is discussed.

### IV. BLIND DETECTION AND ESTIMATION USING MUDE

The signal part in (3) can be decomposed using CPD model [18] with three components as follows

$$\bar{\mathbf{Z}} = \mathbf{G} \circ \mathbf{X} \circ \mathbf{C}. \quad (19)$$

With channel state information unavailable at the receiver, the problem is considered blind. Then the proposed receiver can

fit the CPD model to the received tensor  $\mathcal{Z}$  using alternating least squares (ALS) algorithm, that can be formulated as

$$\hat{\mathbf{G}}, \hat{\mathbf{C}}, \hat{\mathbf{X}} = \underset{\mathbf{G}, \mathbf{C}, \mathbf{X}}{\text{argmin}} \|\mathcal{Z} - \mathbf{G} \circ \mathbf{X} \circ \mathbf{C}\|_F^2, \quad (20)$$

which is equivalent to its matricized forms as follows

$$\hat{\mathbf{G}} = \underset{\mathbf{G}}{\text{argmin}} \|\mathbf{Z}_{(1)} - \mathbf{G}(\mathbf{X} \diamond \mathbf{C})^T\|_F^2, \quad (21)$$

$$\hat{\mathbf{C}} = \underset{\mathbf{C}}{\text{argmin}} \|\mathbf{Z}_{(2)} - \mathbf{X}(\mathbf{G} \diamond \mathbf{C})^T\|_F^2 \quad (22)$$

$$\hat{\mathbf{X}} = \underset{\mathbf{X}}{\text{argmin}} \|\mathbf{Z}_{(3)} - \mathbf{C}(\mathbf{G} \diamond \mathbf{X})^T\|_F^2, \quad (23)$$

where  $\mathbf{Z}_{(n)}$  denotes the  $n$ th matricization of tensor  $\mathcal{Z}$ . Factor matrices  $\mathbf{G}$ ,  $\mathbf{X}$  and  $\mathbf{C}$  can be uniquely determined up to column scaling and permutation if the Kruskal conditions [17], [21] are satisfied, i.e.,  $k_{\mathbf{G}} + k_{\mathbf{X}} + k_{\mathbf{C}} \geq 2U + 2$ . Furthermore, the solutions of the CPD,  $\hat{\mathbf{G}}$ ,  $\hat{\mathbf{C}}$  and  $\hat{\mathbf{X}}$ , can be written as follows

$$\hat{\mathbf{G}} = \mathbf{G}\mathbf{\Pi}\mathbf{\Lambda}_G, \quad \hat{\mathbf{C}} = \mathbf{C}\mathbf{\Pi}\mathbf{\Lambda}_C, \quad \hat{\mathbf{X}} = \mathbf{X}\mathbf{\Pi}\mathbf{\Lambda}_X, \quad (24)$$

where  $\mathbf{\Lambda}_G \mathbf{\Lambda}_C \mathbf{\Lambda}_X = \mathbf{I}_U$ .  $\mathbf{\Pi}$  is the permutation matrix and  $\mathbf{\Lambda}_G$ ,  $\mathbf{\Lambda}_C$  and  $\mathbf{\Lambda}_X$  are column scaling diagonal matrices of  $\mathbf{G}$ ,  $\mathbf{C}$  and  $\mathbf{X}$  respectively. If  $\mathbf{C}$ , the code matrix is assumed to be known at the receiver, then  $\mathbf{C}\mathbf{\Pi}\mathbf{\Lambda}_C = \mathbf{C}$ . Then (24) holds iff  $\mathbf{\Pi} = \mathbf{I}$  and  $\mathbf{\Lambda}_C = \mathbf{I}$ . This is because  $\mathbf{\Pi} = \mathbf{\Lambda}_C^{-1}$ ,  $\mathbf{\Lambda}_C$  is a diagonal matrix and  $\mathbf{\Pi}$  is idempotent. So (24) can now be expressed as

$$\hat{\mathbf{G}} = \mathbf{G}\mathbf{\Lambda}_G, \quad \hat{\mathbf{X}} = \mathbf{X}\mathbf{\Lambda}_X, \quad (25)$$

where  $\mathbf{\Lambda}_G = (\mathbf{\Lambda}_X)^{-1}$ . Since, code matrix  $\mathbf{C}$  is also assumed to be known at receiver, the estimate of the factor matrices  $\mathbf{G}$  and  $\mathbf{X}$  in (21) and (23) for  $j$ th iteration can be computed as

$$\hat{\mathbf{G}}^j = \mathbf{Z}_{(1)}((\hat{\mathbf{X}}^{j-1} \diamond \mathbf{C})^T)^\dagger, \quad (26)$$

$$\hat{\mathbf{X}}^j = [\mathbf{Z}_{(2)}((\hat{\mathbf{G}}^j \diamond \mathbf{C})^T)^\dagger]_{+1/-1}. \quad (27)$$

The matrices derived from (26) and (27) will then undergo only column scaling. Therefore, to identify the factors, each UE may transmit one pilot bit. Scaling factors then can be derived from the first rows of  $\mathbf{X}$  and  $\mathbf{G}$  as given in (25). The matrix  $\mathbf{X}$ , detected by this approach giving  $\hat{\mathbf{X}}$ , is hence iteratively processed through (26) and (27) to extract data symbols.

---

#### Algorithm 1: MUDE receiver algorithm

---

**Input:** Received signal  $\mathcal{Z}$  and user code matrix  $\mathbf{C}$

**Output:** Estimated  $\hat{\mathbf{G}}$  and detected  $\hat{\mathbf{X}}$

- 1 Initialize  $\hat{\mathbf{G}}^0$  and  $\hat{\mathbf{X}}^0$  randomly
  - 2  $j \leftarrow 0$
  - 3 **while**  $\|\hat{\mathbf{G}}^j - \hat{\mathbf{G}}^{j-1}\|_2 \neq 0$  **or**  $\|\hat{\mathbf{X}}^j - \hat{\mathbf{X}}^{j-1}\|_2 \neq 0$  **do**
  - 4      $j \leftarrow j + 1$
  - 5      $\hat{\mathbf{G}}^j \leftarrow \mathbf{Z}_{(1)}((\hat{\mathbf{X}}^{j-1} \diamond \mathbf{C})^T)^\dagger$      // update using (26)
  - 6      $\hat{\mathbf{X}}^j \leftarrow \mathbf{Z}_{(2)}((\hat{\mathbf{G}}^j \diamond \mathbf{C})^T)^\dagger$      // update using (27)
  - 7      $\hat{\mathbf{X}}^j \leftarrow [\hat{\mathbf{X}}^j]_{+1/-1}$      // thresholding
  - 8 **set**  $\hat{\mathbf{X}} = \hat{\mathbf{X}}^j$  and  $\hat{\mathbf{G}} = \hat{\mathbf{G}}^j$
-

This differs from channel estimate utilizing solely pilots, as channel  $\mathbf{G}$  estimation necessitates a minimum of  $MPU$  bits for  $U$  users. In this proposed MUDE algorithm encapsulated in Algorithm 1, each UE is required to transmit only 1 bit, which is fewer than the typical estimation strategies that utilize pilots. The proposed MUDE algorithm exhibits a leading-order computational complexity of  $\mathcal{O}(kMPTQU)$ . In comparison, the zero-forcing (ZF) detector in (5), when combined with a pilot-assisted least squares (LS) channel estimator—referred to as LS-ZF in (29)—yields an asymptotic complexity of the same order as Algorithm 1 with  $k=1$ . However, LS-ZF requires pilot signals and thus incurs a communication overhead that scales proportionally with the number of users  $U$ , whereas the MUDE algorithm operates with a fixed number of  $k$  iterations and consequently a fixed overhead. Moreover, it is important to emphasize that the MUDE algorithm is not sensitive to initialization. The following section presents simulation results that show the efficiency of the proposed MUDE algorithm in CF-mMIMO networks under additive white noise.

## V. SIMULATION RESULTS

### A. Simulation setup

$M = 62$  APs with each of them equipped with  $P = 3$  antennas is considered. Each antenna is assumed to be spaced with  $\lambda/2$ . Number of UE is  $U = 4$ . Each user is sending  $T = 10^3$  bits. The length of the orthogonal code vector ( $Q$ ) is 4. The channel  $\mathbf{g}_{mu} \in \mathbb{C}^3$  between UE  $u$  and antenna  $m$  is modeled as  $\mathcal{CN}(\mathbf{0}_3, \mathbf{R}_{mu})$  where  $\mathbf{R}_{mu}$  is the correlation matrix.  $\mathbf{R}_{mu} = \beta_{mu} \mathbf{I}_3$  and  $\beta_{mu}$  is modeled as in [22]

$$\beta_{mu}(dB) = -30.5 - 36.7 \log_{10}(d_{mu}) + F_{mu}$$

where  $d_{mu}$  (in m) is the distance between user  $u$  and AP  $m$ . Further,  $F_{mu} \sim \mathcal{N}(0, 4^2)$ . Noise  $\mathcal{W}$  is modeled as i.i.d with entries  $\mathcal{CN}(0, \sigma^2)$ . It is assumed that  $\mathbb{E}(\|\mathbf{X}_{tu}\|_F^2) = 1$ .  $d_{um} \leq 1500m$  i.e each user is within  $1500m$  from all the APs. It is also assumed a centralized processing for the system i.e. all computations are done at the CPU. The results are obtained through Monte-Carlo simulations to account for different channel realizations and UE locations. The bit error rate (BER) is used to measure the performance of detection and normalized mean squared error (NMSE) to measure the performance of channel estimation. NMSE between the estimated channel and the true channel and BER was computed respectively as

$$\text{NMSE} = \frac{\mathbb{E}\{\|\mathbf{G} - \hat{\mathbf{G}}\|_F^2\}}{\mathbb{E}\{\|\mathbf{G}\|_F^2\}},$$

$$\text{BER}_{\text{NUM}} = \frac{\sum_{i=1}^T \sum_{j=1}^U \mathbb{I}(\mathbf{X}_{ij} \neq \hat{\mathbf{X}}_{ij})}{TU}.$$

where  $\mathbb{I}$  is the indicator function

### B. State-of-the-art methods

The proposed MUDE algorithm with conventional ZF under both perfect and imperfect channel state information (CSI) scenarios. For perfect CSI, it is assumed that the channel matrix  $\mathbf{G}$  and the orthogonal code matrix  $\mathbf{C}$  are

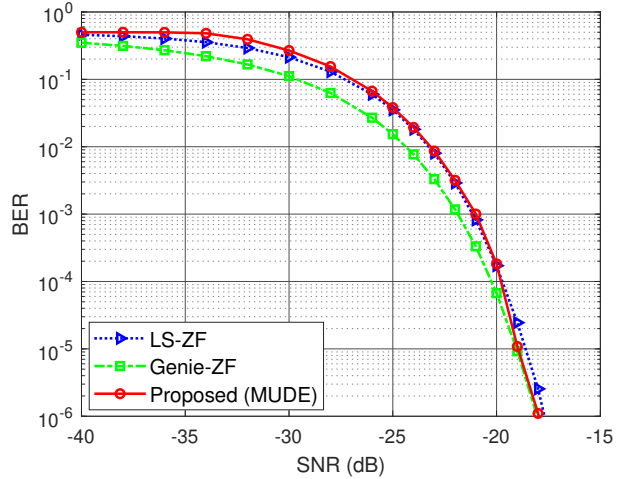


Fig. 2: BER vs. SNR performance comparison of MUDE with LS-ZF (29), Genie-ZF (5) where,  $M = 62$  APs,  $P = 3$  AP antennas,  $U = 4$  users, code length  $Q = 4$  with BPSK.

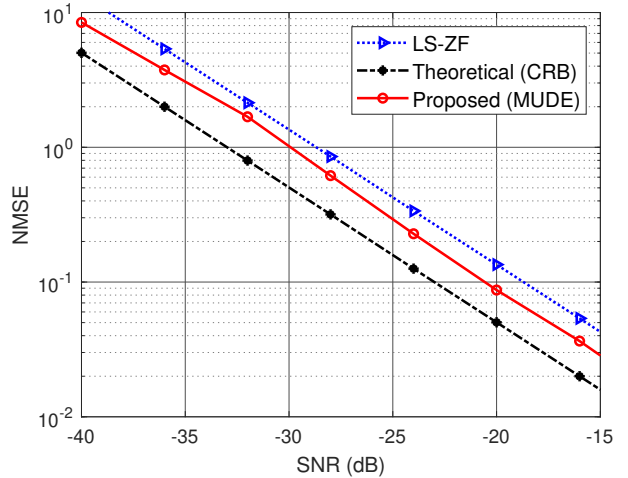


Fig. 3: NMSE vs. SNR performance comparison of MUDE with CRB (17), LS-ZF (28) where,  $M = 62$  APs,  $P = 3$  AP antennas,  $U = 4$  users, code length  $Q = 4$  with BPSK symbols.

completely known, so user data  $\mathbf{X}$  is detected via the second-order matricization as (5). For imperfect CSI, the channel is estimated using least squares by transmitting  $MP$  pilot symbols, gives  $\mathbf{X} = [\mathbf{X}^P, \mathbf{X}^O]$ , where  $\mathbf{X}^P \in \mathbb{R}^{(MP/U) \times U}$  and  $\mathbf{X}^O \in \mathbb{R}^{T-(MP/U) \times U}$  correspond to pilot and data symbols, respectively. The channel is first estimated from pilot observations as

$$\hat{\mathbf{G}}_{LS} = \mathbf{Z}_{(1)}^p ((\mathbf{X}^P \diamond \mathbf{C})^T)^\dagger, \quad (28)$$

after which the remaining data is detected using

$$\hat{\mathbf{X}}_{LS-ZF} = \mathbf{Z}_{(2)}^o ((\hat{\mathbf{G}}_{LS} \diamond \mathbf{C})^T)^\dagger. \quad (29)$$

### C. Result comparisons

The simulations showing the performance of these methods are described here. Fig. 2 depicts the variation of BER vs.

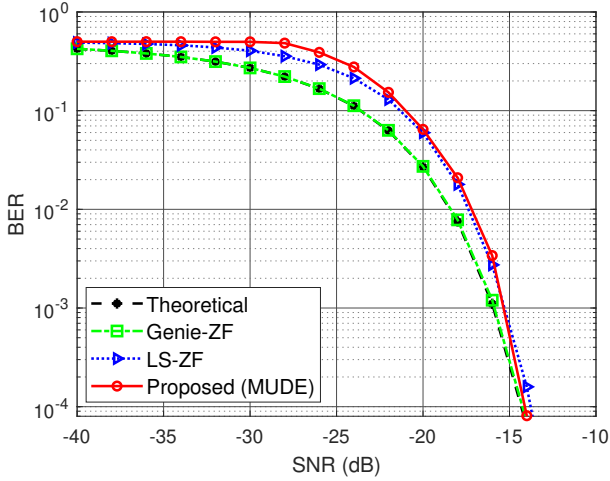


Fig. 4: BER vs. SNR performance comparison of MUDE with minimum PoE (14), Genie-ZF (5), LS-ZF (29) where,  $M = 62$  APs,  $P = 3$  AP antennas,  $U = 2$ , code length  $Q = 1$  with BPSK symbols.

SNR for code length  $Q = 4$  comparing MUDE with Genie-ZF (5) and LS-ZF (29). SNR was varied by changing the noise variance  $\sigma^2$ . Single pilot bit MUDE first overlaps with LS-ZF with  $MP$  pilots and then surpasses and almost achieves the performance of ZF (5) for high SNR values. Fig. 3 depicts the variation of NMSE vs SNR. It is evident from the plot that the pilot based LS-ZF (28) performs with higher NMSE when compared with the MUDE which also explains the better BER performance of the same in Fig. 2.

Fig. 4 depicts the variation of BER vs. SNR, comparing MUDE, Genie-ZF (5) and LS-ZF (29) with the analytical lower bound (12), derived when perfect CSI is available at the receiver with spreading code length 1 and two users. It is evident from the plot that the Genie-ZF almost matches the analytical lower bound derived. The other two techniques are also close to the analytical results for high SNR and is a suitable choice for blind detection and estimation approach.

## VI. CONCLUSION

This work proposed a MUDE algorithm using ALS with one reference/pilot for the uplink CFmMIMO scenario and compared it with two standard techniques: conventional Genie-ZF with perfect CSI at the AP and traditional LS-ZF with imperfect CSI using  $MP$  pilot bits at the AP. The results show that the error gap between MUDE and the theoretical lower bound shrinks as SNR increases. Lower bounds on detection and estimation error for this system are also derived. Although this work does not analyze MUDE's convergence rate and assumes a Rayleigh fading channel, future work will focus on accelerating ALS convergence and extending the analysis to other channel models, such as keyhole and Rician fading.

## REFERENCES

[1] J. Zhang, S. Chen, Y. Lin, J. Zheng, B. Ai, and L. Hanzo, "Cell-free massive mimo: A new next-generation paradigm," *IEEE Access*, vol. 7, pp. 99 878–99 888, 2019.

[2] S. Elhoushy, M. Ibrahim, and W. Hamouda, "Cell-free massive mimo: A survey," *IEEE Communications Surveys & Tutorials*, vol. 24, no. 1, pp. 492–523, 2022.

[3] Z. H. Shaik, E. Björnson, and E. G. Larsson, "Mmse-optimal sequential processing for cell-free massive mimo with radio stripes," *IEEE Transactions on Communications*, vol. 69, no. 11, pp. 7775–7789, 2021.

[4] B. Hassibi and B. M. Hochwald, "How much training is needed in multiple-antenna wireless links?" *IEEE Transactions on Information Theory*, vol. 49, pp. 951–963, 4 2003.

[5] G. Interdonato, E. Björnson, H. Q. Ngo, P. Frenger, and E. G. Larsson, "Ubiquitous cell-free massive communications," *Eurasip Journal on Wireless Communications and Networking*, vol. 2019, 9 2019.

[6] O. Elijah, C. Y. Leow, T. A. Rahman, S. Nunoo, and S. Z. Iliya, "A comprehensive survey of pilot contamination in massive mimo-5g system," *IEEE Communications Surveys and Tutorials*, vol. 18, pp. 905–923, 4 2016.

[7] Z. Luo, C. Li, and L. Zhu, "A comprehensive survey on blind source separation for wireless adaptive processing: Principles, perspectives, challenges and new research directions," *IEEE Access*, vol. 6, pp. 66 685–66 708, 2018.

[8] J. Zhang, X. Yuan, and Y.-J. A. Zhang, "Blind signal detection in massive mimo: Exploiting the channel sparsity," *IEEE Transactions on Communications*, vol. 66, no. 2, pp. 700–712, 2018.

[9] D. D. Souza, M. M. Freitas, G. S. Borges, A. M. Cavalcante, D. B. da Costa, and J. C. Costa, "Effective channel blind estimation in cell-free massive mimo networks," *IEEE Wireless Communications Letters*, vol. 11, no. 3, pp. 468–472, 2021.

[10] X. Huang, X. Zhu, Y. Jiang, and Y. Liu, "Efficient enhanced k-means clustering for semi-blind channel estimation of cell-free massive mimo," in *ICC 2020-2020 IEEE International Conference on Communications (ICC)*. IEEE, 2020, pp. 1–6.

[11] H. He, X. Yu, J. Zhang, S. Song, R. D. Murch, and K. B. Letaief, "Cell-free massive mimo detection: A distributed expectation propagation approach," *IEEE Transactions on Mobile Computing*, 2025.

[12] Z. Zhao and D. Slock, "Hierarchical expectation propagation for semi-blind channel estimation in cell-free networks," *ICASSP, IEEE International Conference on Acoustics, Speech and Signal Processing - Proceedings*, 2025.

[13] C. Xu and P. Comon, "Semi-blind channel estimation in mimo systems," *IEEE Transactions on Signal Processing*, vol. 70, pp. 3508–3522, 2022.

[14] A. Favier and A. L. F. d. Almeida, "Overview of tensor-based cooperative mimo communication systems—part 2: Semi-blind receivers," *Entropy*, vol. 26, no. 11, p. 937, 2024.

[15] J. Li *et al.*, "Tensor-based semi-blind channel estimation for reconfigurable intelligent surface-aided mimo communication systems," *Sensors*, vol. 24, no. 20, p. 6625, 2024.

[16] E. Kofidis, "Revisiting semi-blind block-term decomposition-based receivers for uniform rectangular arrays," *IEEE Workshop on Statistical Signal Processing Proceedings*, pp. 236–240, 2025.

[17] N. D. Sidiropoulos, L. D. Lathauwer, X. Fu, K. Huang, E. E. Papalexakis, and C. Faloutsos, "Tensor decomposition for signal processing and machine learning," *IEEE Transactions on Signal Processing*, vol. 65, pp. 3551–3582, 7 2017.

[18] T. G. Kolda and B. W. Bader, "Tensor decompositions and applications," *SIAM Review*, vol. 51, no. 3, pp. 455–500, 2009.

[19] S. M. Kay, "Statistical signal processing: estimation theory," *Prentice Hall*, vol. 1, pp. Chapter–3, 1993.

[20] X. Liu and N. Sidiropoulos, "Cramer-rao lower bounds for low-rank decomposition of multidimensional arrays," *IEEE Transactions on Signal Processing*, vol. 49, no. 9, pp. 2074–2086, 2001.

[21] J. B. Kruskal, "Three-way arrays: rank and uniqueness of trilinear decompositions, with application to arithmetic complexity and statistics," *Linear Algebra and its Applications*, vol. 18, pp. 95–138, 1 1977.

[22] Ö. T. Demir, E. Björnson, L. Sanguinetti *et al.*, "Foundations of user-centric cell-free massive mimo," *Foundations and Trends® in Signal Processing*, vol. 14, no. 3-4, pp. 162–472, 2021.